

Synthesis and properties of bio-based semi-aromatic heat-resistant copolymer polyamide 5T-co-6T

Xiangcheng Bian^a, Liqun Ma^a, Chen Yang^b, Fuchun Zhang^b, Shuo Zhang^a, Yuan Li^a, Kai Gao^a, Bingxiao Liu^a and Zhongqiang Wang^c

^aDepartment of Materials Engineering, Taiyuan Institute of Technology, Taiyuan, Shanxi, China; ^bResearch and Development Center, Cathay Biotech Inc, Shanghai, China; ^cTechnology center, Guangdong Sinoplast Advanced Material Co. Ltd, Dongguan, Guangdong, China

ABSTRACT

Herein, poly(pentanediamine terephthalamide) (PA5T) homopolymer was synthesized via a salt-forming reaction+solid state polycondensation method using bio-based 1,5-pentanediamine and terephthalic acid as the primary raw materials. To address the issue of its narrower processing window, poly(hexamethylene terephthalamide)(PA6T), which also cannot be melt processed due to the processing window is negative, was introduced into its molecular chain to synthesize poly(pentanediamine/hexanediamine terephthaloyl) (PA5T-co-6T) copolymers. The structures were investigated by Fourier transform infrared spectroscopy (FTIR) and nuclear magnetic resonance carbon spectroscopy (¹³C-NMR). Furthermore, the melting temperature, crystallization temperature, thermal stability, and crystal growth mode of the polymer were tested and analyzed using differential scanning calorimetry (DSC), thermogravimetric analysis (TGA) and wide-angle x-ray diffraction (WAXD), respectively. The results demonstrate that the crystal growth mode gradually changes from three-dimensional spherical growth to two-dimensional disk-like or three-dimensional spherical growth with the increase of 6T chain segment content. Simultaneously, the crystallization temperature, melting temperature, and crystallization rate of the polymer all showed a trend of decreasing first and then increasing, which was due to the combined effects of the increase in the content of 6T chain segments on the molecular-chain structure and crystal structure of the polymer. Bio-based PA5T-co-6T has excellent heat resistance and a wider processing window than PA5T and PA6T, which possesses great application prospects in the fields of automotive, electronic appliances, and LED optics.

ARTICLE HISTORY

Received 28 April 2024
Accepted 6 August 2024

KEYWORDS

Biobased material; heat-resistant material; solid state polymerization; copolymerization modification



Introduction

Polyamide has a regular structure and strong intermolecular forces, which make it easy to crystallize, thus having excellent chemical resistance, wear resistance, and mechanical properties [1,2]. Aliphatic polyamide is produced through the polycondensation of aliphatic diamine and diacid. Its molecular chain is soft and easier to melt process, making it widely used in automotive and electronic fields [3,4]. With the development of surface mount technology (SMT), resins are required to withstand higher reflow soldering temperatures (>270°C) [5]. At the same time, the optical field of LED reflector brackets and new energy vehicles also place higher demands on the heat resistance of resins.

The heat resistance temperature of traditional aliphatic polyamides is below 260°C, which has been difficult to meet the market demands [6]. The fully aromatic polyamide is synthesized through the polycondensation reaction of aromatic diamines and

diacids. It possesses high density of aromatic rings and significant intermolecular forces, making it an extremely heat-resistant material. However, its thermal decomposition onset temperature exceeds its melting point, rendering it ineligible for melt molding processes. Additionally, its high cost restricts its further applications [7,8]. The semi-aromatic polyamide is synthesized through the polymerization of aliphatic diamines with aromatic diacids or vice versa. Its molecular-chain structure features both heat-resistant rigid phenyl rings and flexible aliphatic segments, offering a balance of excellent heat resistance and processability, garnering significant attention [9,10].

Poly(hexamethylene terephthalamide) (PA6T), obtained by polymerization of 1,6-hexanediamine and terephthalic acid (PTA), possesses a high melting temperature, which is exceeding its onset thermal decomposition temperature, making it ineligible for melt

CONTACT Bingxiao Liu  bxliunuc@163.com  Department of Materials Engineering, Taiyuan Institute of Technology, No. 31 Xinlan Road, Jiancaoping District, Taiyuan, Shanxi, China

© 2024 The Author(s). Published by Informa UK Limited, trading as Taylor & Francis Group.

This is an Open Access article distributed under the terms of the Creative Commons Attribution-NonCommercial License (<http://creativecommons.org/licenses/by-nc/4.0/>), which permits unrestricted non-commercial use, distribution, and reproduction in any medium, provided the original work is properly cited. The terms on which this article has been published allow the posting of the Accepted Manuscript in a repository by the author(s) or with their consent.

processing. Furthermore, 1,6-hexanediamine is a petrochemical product. The rapid depletion of fossil resources has adverse effects on the environment, thereby necessitating the substitution of petrochemicals with bio-based materials [11–13].

1,5-pentanediamine and 1,6-hexanediamine have similar structures and can be prepared from lysine through cell biotransformation or direct fermentation from corn [14–16]. And the production capacity of lysine is severely surplus, so developing polyamide (PA5T) based on 1,5-pentanediamine can help digest the production capacity of lysine [17,18]. However, the melting temperature (359.47°C) and thermal decomposition initiation temperature (371.83°C) of PA5T are close to each other, making it easy to decompose during processing. Generally, copolymerizing semi-aromatic polyamide with aliphatic polyamide or introducing flexible segments such as -O- or -S- into the molecular chain can appropriately lower the melting point of the polymer to improve its processability [19,20]. However, there has been no research on modifying the polymer molecular chain and crystal structure by introducing a semi-aromatic 6T chain segment into the PA5T to adjust its processing window.

In this paper, PA5T and PA6T homopolymers were synthesized using 1,5-pentanediamine, 1,6-hexanediamine and PTA as the main raw materials through pre-polymerization and solid-state polycondensation. On this basis, the 6T chain segment was introduced into the main chain of the bio-based PA5T molecule to synthesize a poly(pentanediamine/hexanediamine terephthaloyl) (PA5T-co-6T) copolymer with a wide processing window and excellent heat resistance. The polymer structure was confirmed by Fourier transform infrared spectroscopy (FTIR) and nuclear magnetic resonance carbon spectroscopy (^{13}C -NMR). The melting temperature, thermal decomposition temperature, and processing window of the polymer were characterized by differential scanning calorimetry (DSC) and thermogravimetric analysis (TGA).

Polymer crystallization kinetics is essential for optimizing process conditions, producing high-quality products, and understanding the relationship between polymer structure and properties [21–23]. In particular, non-

isothermal crystallization kinetics is important because in the actual processing and production of polymers, most processes such as extrusion and molding are usually carried out under dynamic non-isothermal conditions [24,25]. The non-isothermal crystallization kinetics parameters and crystal growth mechanism of PA5T, 6T, and 5T-co-6T were analyzed and studied using Jeziorny and Mo methods. The changes in crystal structure were also assessed by wide-angle X-ray diffraction (WAXD).

The preliminary study on the structure, thermal properties, and crystallization mechanism of PA5T/6T copolymers with a wide processing window will effectively promote the engineering application of 5T-based heat-resistant polyamide materials in automotive, electronic appliances, and LED optics.

Materials and methods

Materials

The 1,5-pentanediamine ($\geq 99.5\%$) has been purchased from Cathay Biotech Inc. PTA (≥ 99) and 1,6-hexanediamine ($\geq 99.5\%$) were obtained from Shanghai Aladdin Biochemical Technology Co., Ltd. Sinopharm Chemical Reagent Co., Ltd. provided concentrated sulfuric acid reagent for relative viscosity testing. The deuterated trifluoroacetic acid purchased from Shanghai Ma Kelin Biochemical Technology Co., Ltd. was used as a solvent for ^{13}C -NMR analysis testing. The concentrated sulfuric acid used for testing relative viscosity was bought from Sinopharm Chemical Reagent Co., Ltd. The deionized water used was freshly prepared.

Preparation of PA 5T, 5T-co-6T and 6T salts

Add 1,5-pentanediamine, 1,6-hexanediamine, PTA and proper amount of deionized water into a three necked flask, start stirring, gradually raise the temperature to 40–50°C, react at this temperature for 1.5 h, adjust the PH value of the reaction system to 6.5–7.0, and obtain PA5T, 5T-co-6T and 6T salts (yield $\geq 90\%$). The specific formula of raw materials is shown in Table 1.

Table 1. Composition of PA 5T, 5T-co-6T and 6T.

Samples (PA)	1,5-pentanediamine/mol	1,6-hexanediamine/mol	PTA/mol	H ₂ O/wt%
5T	1.00	–	1.00	30
5T/6T-0.2	0.80	0.20	1.00	30
5T/6T-0.4	0.60	0.40	1.00	30
5T/6T-0.5	0.50	0.50	1.00	30
5T/6T-0.6	0.40	0.60	1.00	30
5T/6T-0.8	0.20	0.80	1.00	30
6T	–	1.00	1.00	30

Synthesis of PA 5T, 5T-co-6T and 6T

Add PA 5T, 5T-co-6T or 6T salts to the high-temperature high-pressure polymerization reactor, purge the reactor with inert gas for 5–10 min to make the polymerization reaction system an inert gas atmosphere, and then start programmed temperature rise. Within 2 h, the heating temperature of the polymerization reaction system is increased to 220–230°C, during which the polymerization pressure gradually increases. After the pressure in the polymerization reactor rises to 2.0 MPa, gradually release the pressure to negative pressure within 1 h, while continuing to increase the temperature of the polymerization reaction system to 240°C. Under these temperature and pressure conditions, the reaction was sustained for 2 h to obtain PA 5T, 5T-co-6T, and 6T, respectively.

Testing and characterization of PA 5T, 5T-co-6T and 6T

First, the fixed-mass PA5T and PA5T-co-6T samples were dissolved in equal volumes of concentrated sulfuric acid. After the samples dissolved, the flow times of concentrated sulfuric acid and different formulations of polymer solutions were measured using an Ubbelohde viscometer. The relative viscosity of the sample is obtained by the ratio of the flow time of polymer solutions with different formulations to concentrated sulfuric acid.

The FTIR was obtained using an IS50 infrared absorption spectrometer from Thermo Nicolet. A suitable amount of polymer powder was mixed with potassium bromide and compressed into a tablet, which was then placed in the instrument for scanning. The test mode was TR, and the scanning range was 4000–500 cm^{-1} .

A small amount of polymer sample was dissolved in deuterated trifluoroacetic acid, and the polymer structure was confirmed using a Bruker DPX-400 NMR spectrometer (frequency 400 MHz).

The 3–10 mg samples were placed in a crucible and tested with a DSC (Q20, TA). The temperature was initially raised above the melting point of the polymer at a rate of 40°C/min, and maintain for 5 min to eliminate thermal history, then cool down to room temperature at rates of 5, 10, 20, and 40°C/min, respectively, and hold at room temperature for 5 min, then heat up again to above the polymer melting temperature at a rate of 10°C/min, record the DSC curves.

The TGA curves of the sample were tested using a Q2000 instrument from TA Corporation. The atmosphere was N_2 , the heating rate was 10°C/min, and the temperature range was 30–700°C.

The WAXD diffraction pattern was obtained using a TD-3700 instrument with a testing range of 3–60° and a scanning rate of 3°/min.

Results and discussion

Relative viscosity analysis of 5T, 5T-co-6T, and 6T salts and PA5T, 5T-co-6T, and 6T

The relative viscosity values of PA5T, PA5T-co-6T, and PA6T are shown in Table 2. It can be seen from Table 2 that polymers with different formulations all have relatively high relative viscosity, and the relative viscosity values between different samples do not vary significantly.

Figure 1(a,b) are the FTIR spectra of 5T, 5T-co-6T, 6T salts and PA 5T, 5T-co-6T, 6T, respectively. In Figure 1(a), the peak near 2141 cm^{-1} is the frequency doubling absorption peak of NH^{3+} in the polyamide salt, and the peak near 744 cm^{-1} is the telescopic vibration absorption peak of OH. As shown in Figure 1(b), the peaks located near 2932 cm^{-1} and 2855 cm^{-1} are the telescopic vibration absorption peaks of the methylene ($-\text{CH}_2-$) in polyamide. The amide I to amide V bands are located near 1624 cm^{-1} (amide I band, C=O telescopic vibration absorption peak), 1544 cm^{-1} (amide II band, N-H in-plane bending vibration absorption peak and C-N telescopic vibration absorption peak), 1279 cm^{-1} (amide III band, C-N telescopic vibration absorption peak and C-H in-plane bending vibration absorption peak), 1013 cm^{-1} (amide IV band, C-CO telescopic vibration absorption peak), and 730 cm^{-1} (amide V band, CH_2 rocking vibration absorption peak) [26–28]. In addition, it can be found that the frequency doubling absorption peak of NH^{3+} in the polyamide salt near 2141 cm^{-1} in Figure 1(a) does not appear in the infrared spectrum of the polymer (Figure 1(b)), proving that PA 5T, 5T-co-6T and 6T polymers were indeed synthesized.

^{13}C -NMR analysis of PA 5T, 5T-co-6T, and 6T

Figure 2 shows the ^{13}C -NMR spectras of PA 5T, 5T-co-6T and 6T. As shown in Figure 2, the chemical shifts at near 171.0 ppm correspond to the carbon atom on the

Table 2. Relative viscosity of PA5T, PA5T-co-6T and PA6T.

Samples(PA)	5T	5T-co-6T-0.2	5T-co-6T-0.5	5T-co-6T-0.8	6T
Relative viscosity	1.46	1.52	1.39	1.40	1.38

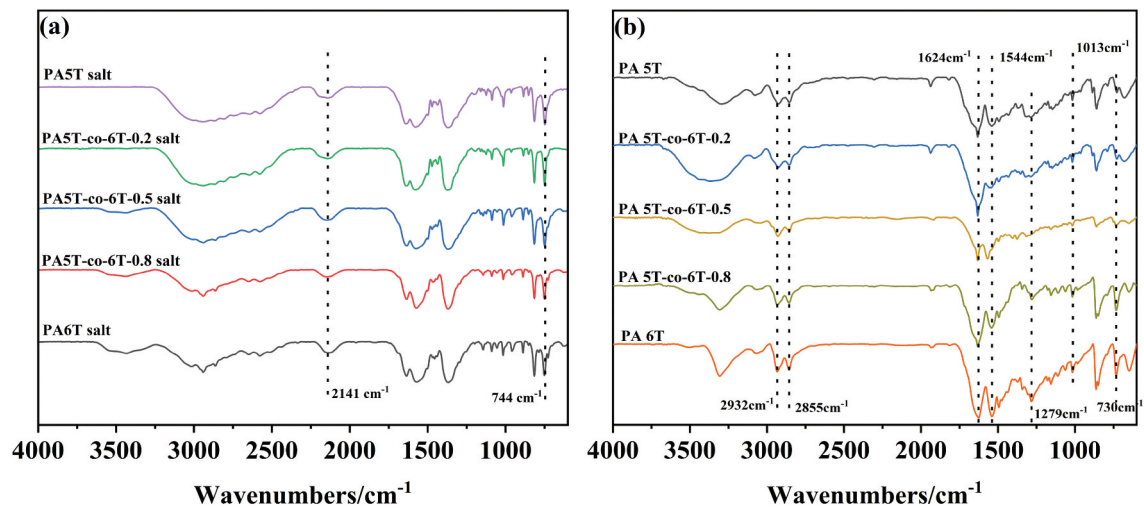


Figure 1. Infrared spectra of 5T, 5T-co-6T, 6T salts(a) and PA5T, 5T-co-6T, 6T(b).

carbonyl group (position a). The peak at approximately 134.7 ppm originates from the carbon atom on the phenyl ring attached to the carbonyl group (position b). The chemical shifts at 127.6 ppm are attributed to carbon atom at position C of the benzene ring (position c), and the peak near 41.2 ppm is the peak corresponding to the carbon atom on the methylene group attached to the N atom of the amide group (position d). The proton signals of the carbon atoms on other methylene groups except for the methylene group mentioned above are in the range of 27.5 to 22.5 ppm (positions e and f). It is worth noting that, as shown in Figure 2(b) (a partial enlarged view of positions b and d in Figure 2(a)), in position b, both PA5T and PA6T have a single peak, while PA5T-co-6T has multiple peaks, which is caused by the random copolymerization of 5T and 6T chain

segments, consistent with existing literature reports [29]. In position d, the position of the PA6T peak(d') is slightly shifted compared to the position of the PA5T peak (d). For PA5T-co-6T, as the content of 6T segment increases, the peak at d' position becomes more obvious, while the peak at d position gradually decreases until disappearing. The height of d' and d peaks represents the ratio of 6T segment to 5T segment in the polymer. The positions of these peaks are consistent with the theoretical peak positions of PA5T, 5T-co-6T, and 6T, confirming their structures.

Differential scanning calorimetry analysis

Figure 3 shows the melting curves of PA 5T, 5T-co-6T, and 6T. As depicted in Figure 3(a), the melting temperature

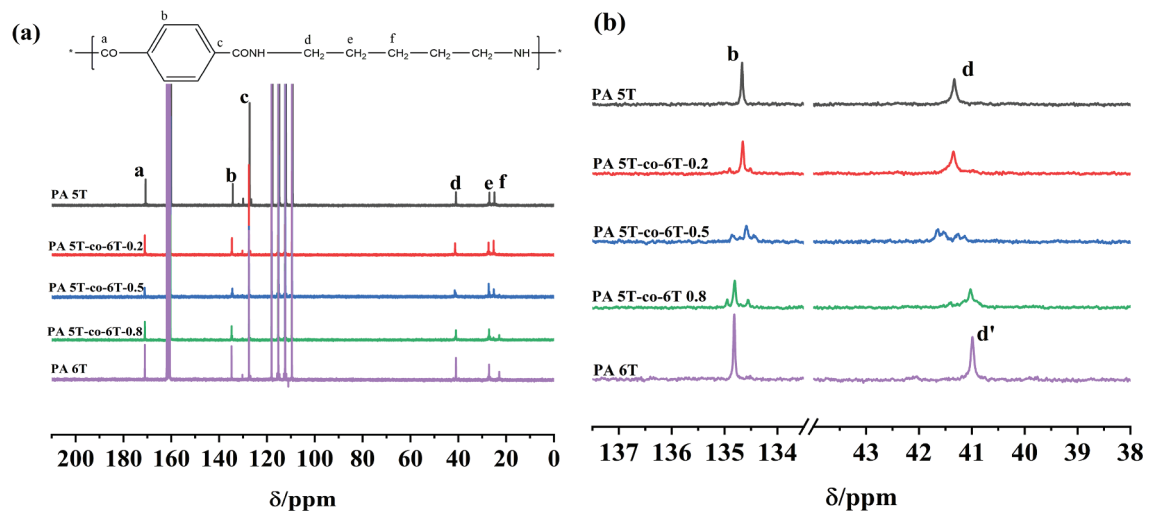


Figure 2. ¹³C NMR spectrum of nylon 5T, 5T-co-6T, 6T (a) and partial enlarged view (b).

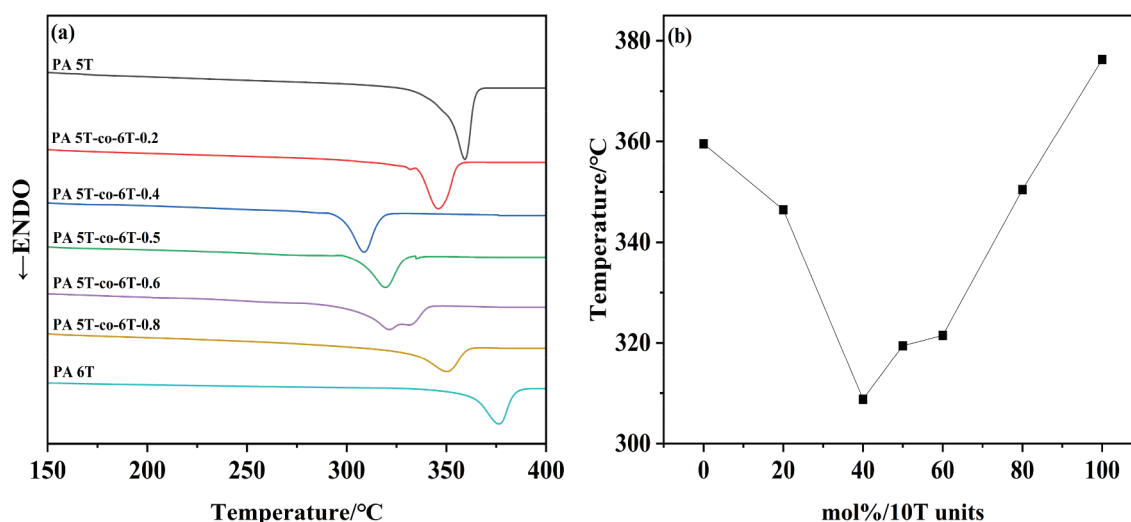


Figure 3. DSC curves of PA 5T, 5T-co-6T and 6T.

of PA5T is 359.25°C, which is lower than that of PA6T (376.69°C). This is because although the molecular chain of PA5T is shorter and the density of rigid benzene rings is higher, 1,5-pentanediamine is a diamine with odd carbon atoms, while hexanediamine is a diamine with even carbon atoms. Under the same conditions, the hydrogen bond density of polyamides formed by diamine with even carbon atoms is higher than that of diamine with odd carbon atoms. Compared with PA6T, PA5T has a much lower hydrogen bond density and weaker intermolecular forces, but the density of benzene rings is not much different between the two. The intermolecular hydrogen bond force plays a dominant role in determining the melting temperature of both, so PA6T has a higher melting temperature than PA5T. Moreover, it can be observed from Figure 3(b) that as the content of the 6T chain segment increases, the polymer's melting temperature exhibits a pattern of initially decreasing and then increasing trend. When the proportion of 6T chain segment is 40%, the copolymer has the lowest melting temperature (308.73°C). This is because when the content of the 6T chain segment is small, the addition of the 6T chain segment disrupts the regularity of the PA5T molecular chain, and the 6T chain segment exists as a crystal defect, resulting in a decrease in the melting temperature of the copolymer, which is consistent with the current copolymerization modification studies [30–33]. When the proportion of 6T chain segment is greater than 40%, the melting temperature of the polymer shows a gradual increase, especially when the proportion of 6T chain segment reaches 80%, the melting temperature of the copolymer increases significantly. This is because on the one hand, with the further increase in the content of 6T chain segments, they gradually become the main molecular

chain, and the molecular-chain regularity of the polymer becomes relatively better. On the other hand, the hydrogen bond density and intermolecular force of 6T chain segments are greater than those of 5T. These two factors lead to a gradual increase in the melting temperature of the polymer.

Thermogravimetric analysis

The TGA and differential thermogravimetric (DTG) curves of PA 5T, 5T-co-6T and 6T are depicted in Figure 4(a,b) respectively. As can be seen from the Figures, the introduction of the 6T chain segment does not affect the thermal decomposition initiation temperature and maximum thermal decomposition rate temperature of the copolymer, all have extraordinary heat resistance. At the same time, the processing window (thermal decomposition initiation temperature minus melting temperature value) of polymers with different 6T chain segment contents is listed in Figure 4(c). It can be clearly seen that the PA5T-co-6T copolymer has a wider processing window than both PA5T and PA6T homopolymers.

Non-isothermal crystallization analysis

Non-isothermal crystallization behaviors of PA 5T, 5T-co-6T, and 6T

Figure 5 displays the crystallization curves of PA 5T, 5T-co-6T, and 6T at different cooling rates. The crystallization temperatures of PA 5T, 5T-co-6T, and 6T at different cooling rates are provided in Table 3. As shown in Figure 5, all curves exhibit a single peak, and as the cooling rate increases, the crystallization peak temperature of all

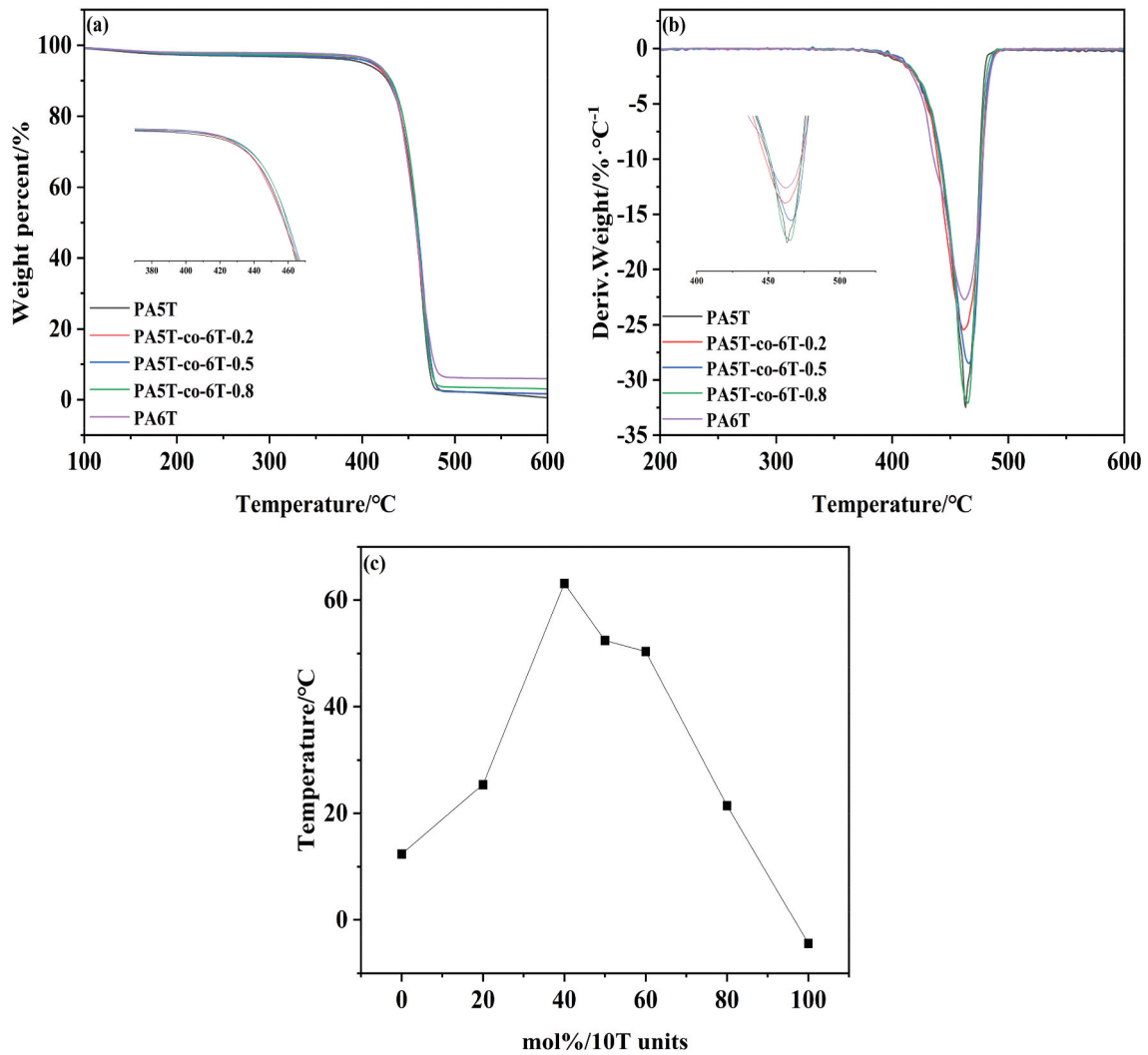


Figure 4. TGA (a) and DTG (b) curves, and processing window versus mol% 6T chain segment (c).

samples decreases and the peak shape broadens, which is a common phenomenon for semi-crystalline polyamide. This is mainly due to the fact that the crystallization of polymers involves two stages: the formation of crystal nuclei and the growth of crystals [34–36]. When the cooling rate is high, the molecular chains do not have enough time to overcome the barriers at higher temperatures to form an ordered arrangement, so the crystallization temperature decreases. As for the broadening of the peak shape, it is because the molecular chain has a strong ability to move and is easier to arrange into a regular structure at high temperature. However, the samples with a higher cooling rate have a shorter residence time at both high and low temperatures, and the crystal nuclei and crystals do not have sufficient time to form and grow. Therefore, the rate of imperfect crystals is higher, resulting in a widening of the crystallization peak shape.

From Table 3, it can also be seen that at the same cooling rate, with the increase of the 6T chain segment

content, the crystallization temperature of the copolymer first decreases and then increases, consistent with the trend of the melting temperature. This is due to the gradual deterioration and then improvement of the regularity of the polymer molecular chain with the addition and gradual increase of the 6T segment content.

Crystallization kinetics analysis of PA 5T, 5T-co-6T, and 6T

The relative crystallinity of a polymer can be determined by the ratio of the area of the crystallization curve formed at a certain crystallization temperature to the area of the entire crystallization peak. Equation (1) illustrates the relationship between relative crystallinity X_T and T .

$$X_T = \frac{\int_{T_0}^T \frac{d(T)}{d(T)}}{\int_{T_0}^{T_\infty} \frac{dH_c(T)}{d(T)}} \quad (1)$$

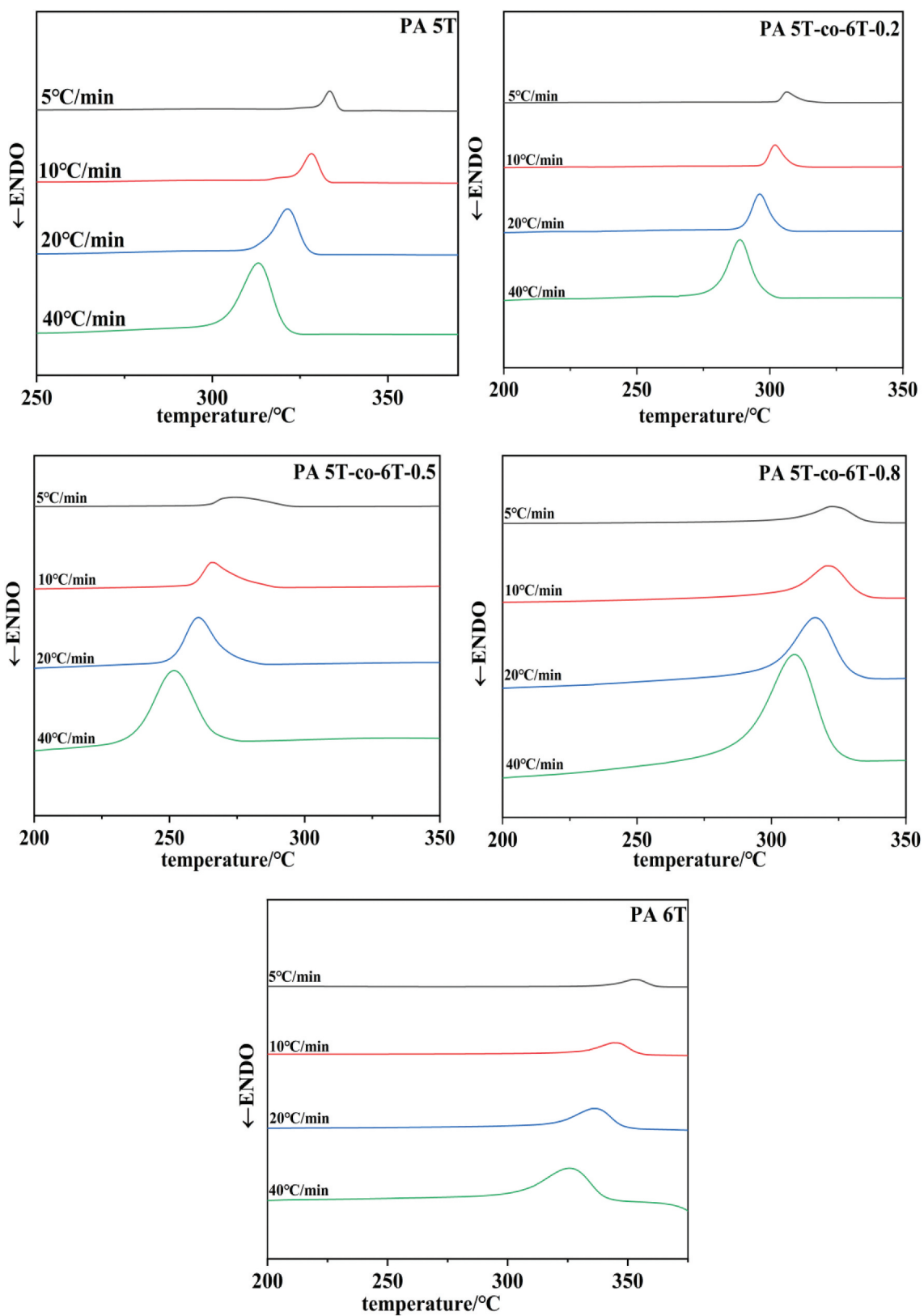


Figure 5. Non-isothermal crystallization curves of PA5T, 5T-co-6T and 6T.

Table 3. Non-isothermal crystallization parameters of PA 5T, 5T-co-6T and 6T.

Sample	$\phi/^\circ\text{C}\cdot\text{min}^{-1}$	$T_p/^\circ\text{C}$	$T_{1/2}/\text{min}$	G
PA 5T	5	333.31	0.88	1.14
	10	328.49	0.63	1.60
	20	321.41	0.48	2.09
	40	313.31	0.33	3.02
PA 5T-co-6T-0.2	5	306.22	2.58	0.39
	10	301.95	1.14	0.88
	20	296.41	0.65	1.54
	40	289.16	0.39	2.53
PA 5T-co-6T -0.5	5	273.73	3.75	0.27
	10	266.04	2.13	0.47
	20	260.43	1.12	0.89
	40	252.46	0.56	1.80
PA 5T-co-6T-0.8	5	323.29	2.83	0.35
	10	321.78	1.72	0.58
	20	316.21	1.05	0.95
	40	308.37	0.49	2.06
PA 6T	5	352.69	2.10	0.48
	10	346.55	1.31	0.76
	20	337.29	0.85	1.17
	40	326.52	0.47	2.14

In the formula, T_0 represents the initial crystallization temperature, T is the crystallization temperature corresponding to a specific moment t , and T_∞ is the termination crystallization temperature. Figure 6. shows the relative crystallinity of PA5T, 5T-co-6T, and 6T versus temperature at different cooling rates. As indicated in Figure 6., all curves exhibit inverse S shapes, and the crystallization onset temperature and the corresponding temperature at a given relative crystallinity both decrease with increasing cooling rate, which is due to the hysteresis effect of crystal formation.

In the non-isothermal crystallization process, the crystallization time t and crystallization temperature T can be converted according to equation 2:

$$t = \frac{T_0 - T}{\phi} \quad (2)$$

Where ϕ corresponds to the cooling rate. According to equations 1 and 2, the curves of relative crystallinity versus time are presented in Figure 7. The time $t_{1/2}$ corresponding to 50% relative crystallinity can be obtained from the graph. The crystallization rate constant is $G = (t_{1/2})^{-1}$. $t_{1/2}$ and G values of all samples at different cooling rates are listed in Table 3. Generally, a larger G value represents a faster crystallization rate. It can be clearly seen from Table 3 that at the same cooling rate, the G value of PA5T is greater than that of PA6T, indicating that the crystallization rate of PA5T is higher than that of PA6T. This is because although the longer molecular chain of PA6T results in relatively better flexibility of its molecular chain, the greater hydrogen bonding effect of PA6T limits the mobility of the molecular chain to a certain extent. The above reasons lead to a slower crystallization rate of PA6T compared to PA5T,

which is consistent with the above analysis of the melting temperature (the melting temperature of PA5T is lower than that of PA6T). It can also be found from Table 3 that at the same cooling rate, the G value of the copolymer decreases first and then increases with the increase of the 6T chain segment content, representing a slowing down and then speeding up of the crystallization rate. This is due to the fact that when the 6T chain segment content is small, the 6T chain segment exists as a crystal defect, and the addition of the 6T segment disrupts the regularity of the molecular backbone, thus slowing down the crystallization rate. However, when the 6T segment content continues to increase, the 6T chain segment gradually becomes the molecular backbone, and the regularity of the polymer is improved again, thus the crystallization rate is accelerated.

Analysis of the jeziorny method

Assuming that the crystallization temperature is constant, the primary stage of the crystallization process can be described by Avrami equation:

$$X_t = 1 - \exp(-Z_t t^n) \quad (3)$$

$$\lg[-\ln(1 - X_t)] = n \lg t + \lg Z_t \quad (4)$$

Where X_t is the relative crystallinity, n corresponds to the Avrami index, t and Z_t are the time corresponding to a given relative crystallinity and the crystallization rate constant, respectively. Considering the non-isothermal characteristics of the crystallization process, Z_t is modified in the Jeziorny method as follows:

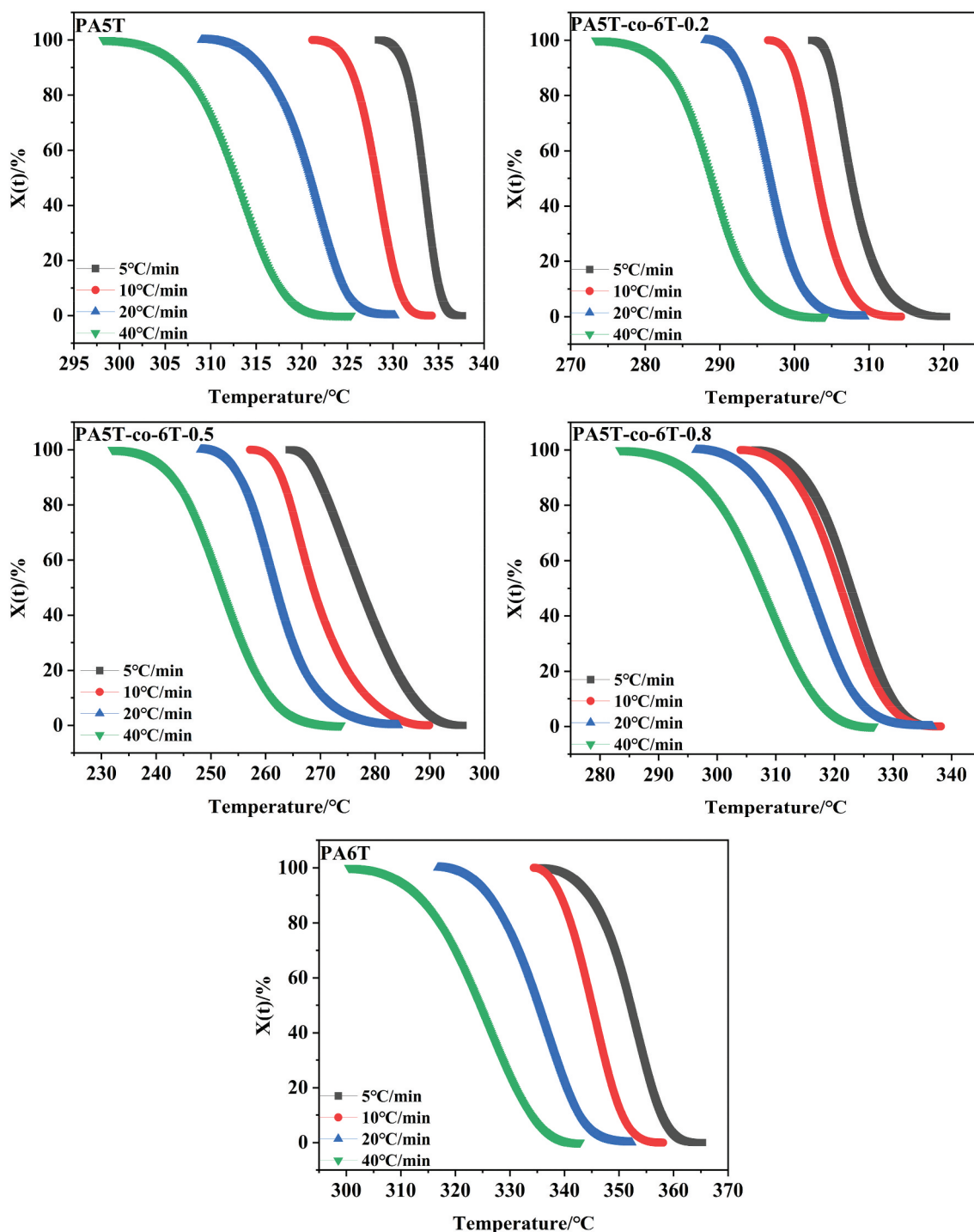


Figure 6. Relative crystallinity versus temperature curves of PA 5T, 5T-co-6T and 6T.

$$\lg Z_c = \frac{\log Z_t}{\varphi} \quad (5)$$

Where Z_c and φ denote the modified crystallization rate constant and the cooling rate. Figure 8 presents the curves of $\lg[-\ln(1 - X_t)]$ versus $\lg t$. The values of n can be obtained by fitting the slope of the line, and Z_c can be calculated by intercept, which are all listed in Table 4.

Table 4 also presents the correlation coefficient R^2 of the fitted lines. Interestingly, it can be observed that the n values of PA 5T and PA 5T-co-6T-0.2 are in the range of 3–4, whereas the n values of PA5T-co-6T-0.5, PA 5T-co-6T-0.8 and PA 6T are in the range of 2–4. This indicates that the crystal growth mode of PA 5T and PA 5T-co-6T-0.2 is three-dimensional spherical growth, while as the content of 6T chain increases, the crystal growth mode

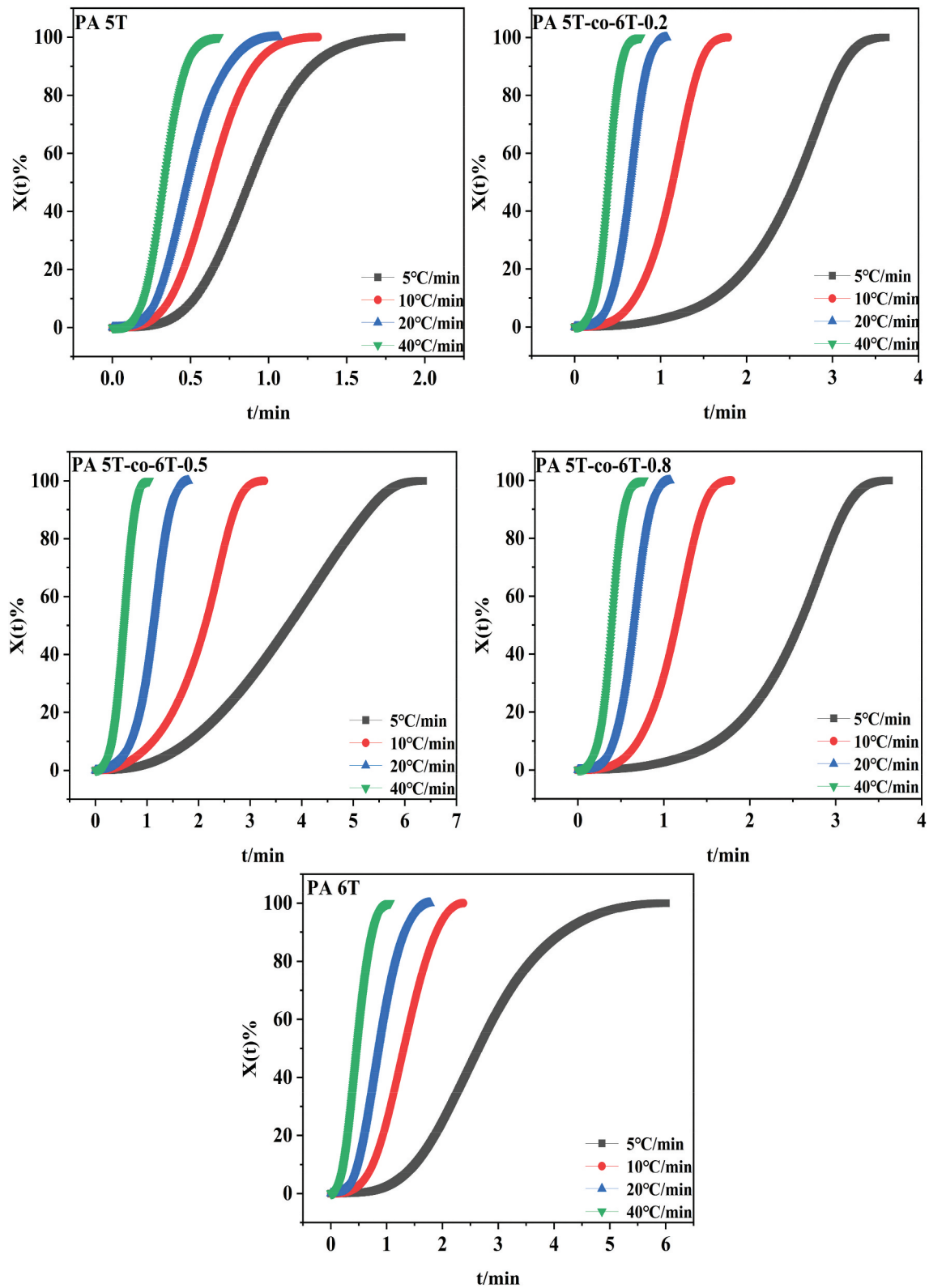


Figure 7. Relative crystallinity versus time curves of PA 5T, 5T-co-6T and 6T.

gradually changes to two-dimensional disk or three-dimensional spherical growth. In addition, according to Table 3, the value of Z_c decreases first and then increases with the increase of the content of 6T chain

segments. Generally, a higher Z_c value indicates a faster crystallization rate, which is consistent with the analysis results of the above-mentioned crystallization rate constant G value.

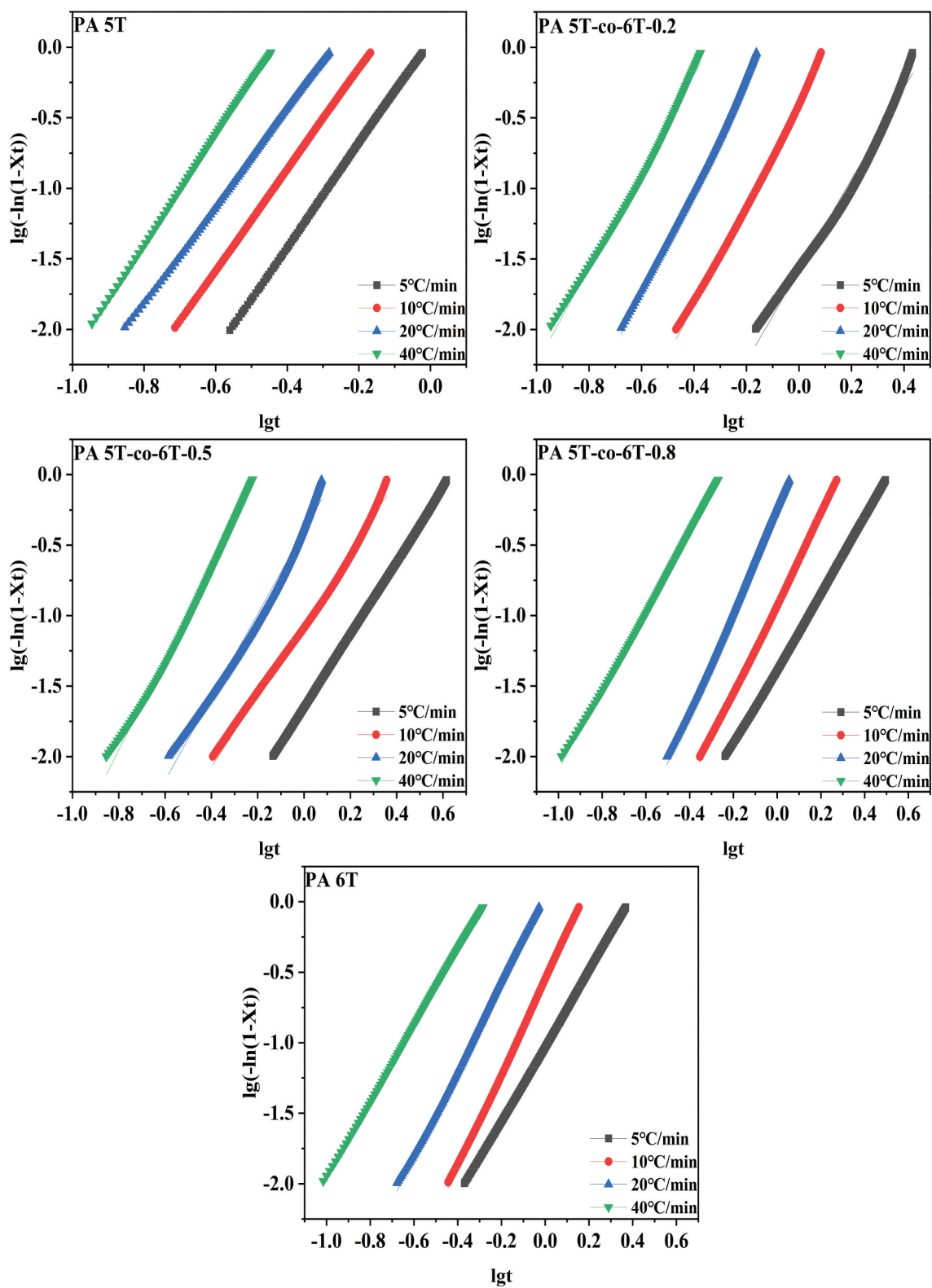


Figure 8. Plots of $\log[-\ln(1-X_t)]$ versus $\lg t$ for PA 5T, 5T-co-6T and 6T.

Table 4. Crystallization kinetics parameters determined by Jeziorny method.

Sample	$\varphi/^\circ\text{Cmin}$	n	Z_c	R^2
PA 5T	5	3.68	1.03	1.00
	10	3.59	1.14	1.00
	20	3.47	1.12	1.00
	40	3.89	1.10	1.00
PA 5T-co-6T-0.2	5	3.23	0.48	0.99
	10	3.56	0.91	1.00
	20	3.76	1.06	1.00
	40	3.42	1.07	0.99
PA 5T-co-6T-0.5	5	2.59	0.47	1.00
	10	2.54	0.78	0.99
	20	2.95	0.96	0.99
	40	3.24	1.04	1.00
PA 5T-co-6T-0.8	5	2.71	0.53	1.00
	10	3.18	0.81	1.00
	20	3.61	0.97	1.00
	40	2.80	1.04	1.00
PA 6T	5	2.68	0.62	1.00
	10	3.33	0.88	1.00
	20	3.11	1.01	1.00
	40	2.70	1.04	1.00

Mo method analysis

The Ozawa equation is suitable for analyzing a remarkably narrow range of crystallization temperatures, and thus cannot describe the entire non-isothermal crystallization process. Mo et al. proposed an ideal method for investigating the non-isothermal crystallization process by combining the Avrami and Ozawa equations [37–41].

$$\lg Z_t + n \lg t = \lg K(T) - m \lg \varphi \quad (6)$$

$$\lg \varphi = \lg F(T) - \alpha \lg t \quad (7)$$

Where m is the Ozawa index, $\alpha = n/m$ and $F(T)$ represents the cooling rate required to reach a certain relative crystallinity per unit time, and its value can reflect the speed of the polymer crystallization rate: larger values indicate lower crystallization rates. According to equation (7), the plots of $\lg \varphi$ against $\lg t$ are presented in Figure 9., which exhibits high correlation coefficient (the $R^2 \geq 0.95$, Table 4), indicating that the Mo method could be used to analyze the non-isothermal crystallization process of PA5T, 5T-co-6T and 6T. Moreover, the values of α and $F(T)$ could be obtained from fitting the slope and intercept of the lines, respectively, which are presented in Table 5. Interestingly, at any given relative crystallinity, as the 6T segment content increases, the $F(T)$ value first increases and then decreases, indicating that the crystallization rate of the polymer first decreases and then increases during the entire crystallization process, which is consistent with the results of Jeziorny's method analysis.

WAXD analysis

The WXR patterns of 5T, 5T-co-6T, 6T salts, and PA5T, 5T-co-6T, 6T are displayed in Figure 10a and 10b, respectively. As indicated Figure 10a., the peak positions of PA5T salt are at 15.25°, 21.15°, 25.27°, 26.13° and 27.16°, which is consistent with the literature reports on monohydrate form salts. In addition, the peaks at 21.15° and 27.16° gradually decrease until they disappear as the content of the 6T chain segment increased to 50%. Significantly, when the content of the 6T chain segment reaches 60% and continues to increase, the peak at 25.60° gradually increases, indicating that the crystallization area of the 5T salt decreases, while the crystallization area of the 6T salt increases Figure 10b shows that the peaks at 6.85°, and 21.15° gradually disappeared, and the peaks at 22.95°, and 25.71° gradually appeared and increased with the increase in the content of the 6T chain segment, which represent the decrease in the crystalline region of PA 5T, and the formation of the crystalline region of PA6T.

Conclusions

PA5T, 5T-co-6T, and 6T were synthesized using the salt formation + solid-phase polymerization. On this basis, the influence of 6T chain segment on the polymer molecular-chain structure, thermal properties, non-isothermal crystallization kinetics, and crystal structure were investigated. The study found that with the increase of the 6T chain segment content, the melting temperature, crystallization temperature, and crystallization rate of the polymer all showed a trend of first decreasing and then increasing, and the crystal growth

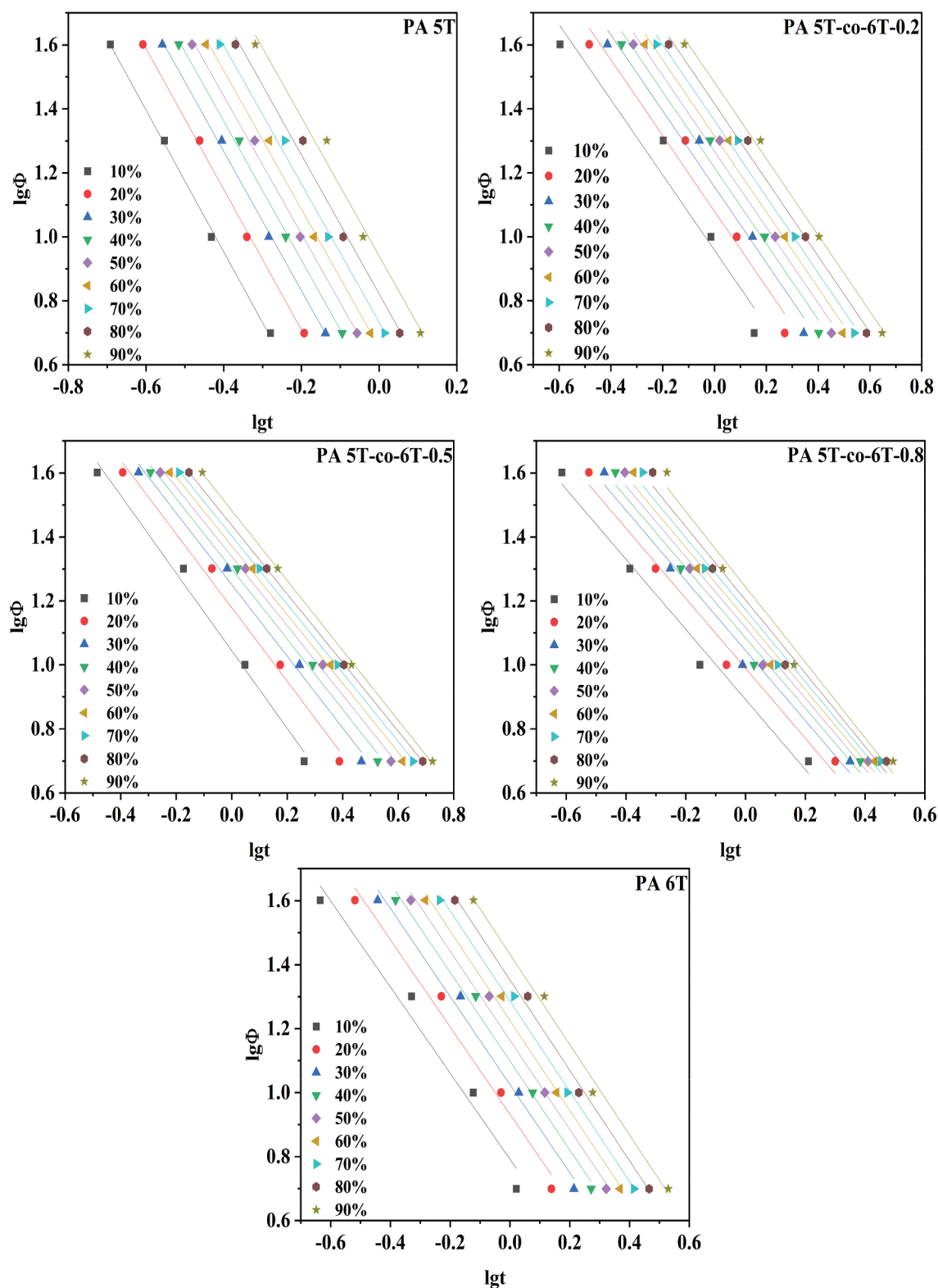


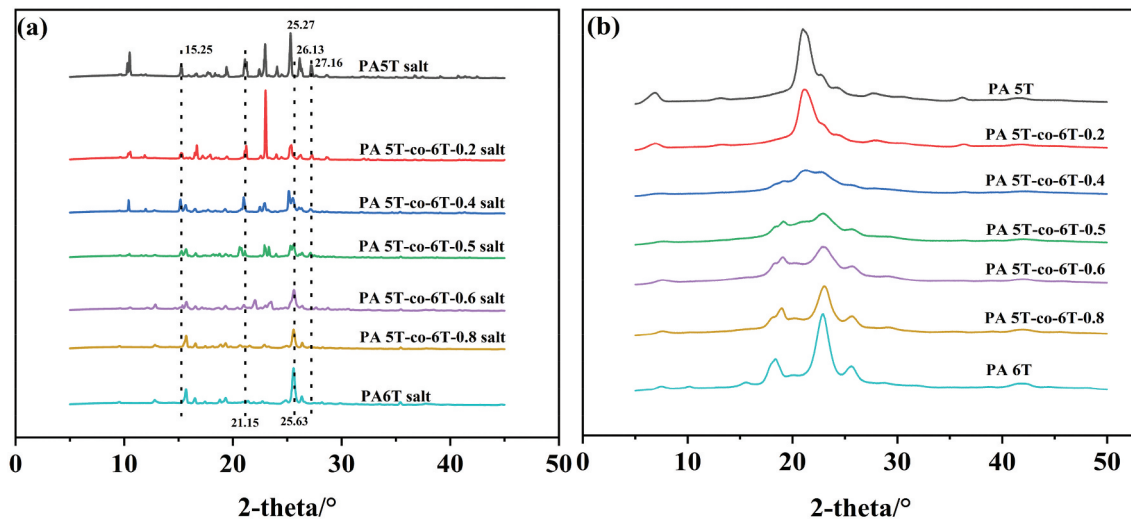
Figure 9. Plots of $\lg\phi$ versus $\lg t$ for PA 5T, 5T-co-6T and 6T.

mode shifted from three-dimensional spherical to two-dimensional disk-like or three-dimensional spherical growth, which was due to the influence of the addition

of 6T chain segment on the polymer molecular-chain structure and crystal structure. Compared with PA 5T and 6T homopolymers, PA 5T-co-6T has a broader

Table 5. Crystallization kinetics parameters obtained by Mo method.

Sample	$X(t)/\%$	α	$F(t)$	R^2
PA 5T	10	2.21	1.17	0.99
	20	2.20	1.86	0.99
	30	2.18	2.49	0.99
	40	2.17	3.11	0.99
	50	2.16	3.79	0.99
	60	2.16	4.51	0.99
	70	2.16	5.41	0.99
	80	2.17	6.63	0.99
	90	2.17	8.72	0.99
PA 5T-co-6T-0.2	10	1.10	7.80	0.99
	20	1.09	9.76	0.99
	30	1.10	11.09	0.99
	40	1.10	12.15	0.99
	50	1.11	13.08	0.99
	60	1.11	13.96	0.99
	70	1.13	14.88	0.99
	80	1.15	15.96	0.99
	90	1.18	17.53	0.98
PA 5T-co-6T-0.5	10	1.21	11.08	0.99
	20	1.15	15.11	0.99
	30	1.12	17.83	0.99
	40	1.10	19.98	0.99
	50	1.08	21.82	0.99
	60	1.08	23.57	0.99
	70	1.07	25.32	0.99
	80	1.07	27.32	0.99
	90	1.08	30.38	0.99
PA 5T-co-6T-0.8	10	1.18	9.07	0.95
	20	1.18	12.01	0.97
	30	1.19	14.32	0.98
	40	1.19	16.43	0.98
	50	1.18	18.48	0.99
	60	1.19	20.65	0.99
	70	1.19	23.06	0.99
	80	1.19	26.02	0.99
	90	1.19	30.34	0.99
PA 6T	10	1.35	6.19	0.96
	20	1.36	8.56	0.98
	30	1.38	10.59	0.98
	40	1.39	12.55	0.99
	50	1.39	14.57	0.99
	60	1.40	16.79	0.99
	70	1.41	19.32	0.99
	80	1.41	22.51	0.99
	90	1.41	27.09	0.99

**Figure 10.** XRD patterns of PA 5T, 5T-co-6T, 6T salts(a) and PA 5T, 5T-co-6T, 6T(b).

processing window and good heat resistance, making it a bio-based heat-resistant engineering plastic with more excellent potential application value.

Acknowledgments

We would like to express our gratitude to Dr Yang Chen from Cathay Biotech Inc. for his guidance on the experimental protocol, and to Dr Wang Zhongqiang from Guangdong Zhongshu New Materials Co., Ltd for his support in performance testing and data analysis.

Disclosure statement

No potential conflict of interest was reported by the author(s).

Funding

This work is sponsored by Fundamental Research Program of Shanxi Province (free exploration) [202303021222305], Taiyuan Open bidding for selecting the best candidates project [2024TYJB0145], Shanxi Provincial Key Research and Development Project [202102040201005] and Taiyuan Institute of Technology Talent Introduction Research Funding Project (2022KJ045).

Availability of data and material

The original data of this research paper can be requested from the corresponding author.

References

- [1] Zhang C. Progress in semicrystalline heat-resistant polyamides. *e-Polymers*. 2018;18(5):373–408. doi: [10.1515/epoly-2018-0094](https://doi.org/10.1515/epoly-2018-0094)
- [2] Wang Z, Lin N, Kang H, et al. Miscibility, crystallization and properties of bio-based polyamide 56/polyamide 6 blends. *Polymer*. 2023;265. doi: [10.1016/j.polymer.2022.125603](https://doi.org/10.1016/j.polymer.2022.125603)
- [3] Zhang G, Y-X Z, Kong Y, et al. Semiaromatic polyamides containing ether and different numbers of methylene (2–10) units: synthesis and properties. *RSC Adv*. 2014;4(108):63006–63015. doi: [10.1039/C4RA10074C](https://doi.org/10.1039/C4RA10074C)
- [4] G-M Y, Zhang G, H-H R, et al. Synthesis and characterization of semiaromatic polyamides with dicyclohexane units. *RSC Adv*. 2016;6(80):76490–76497. doi: [10.1039/C6RA13021F](https://doi.org/10.1039/C6RA13021F)
- [5] Costantino G. Advances in polyamide 4T for lead free solder surface mount technology (SMT) applications. SAE technical paper series. 2013. doi: [10.1002/pola.28983](https://doi.org/10.1002/pola.28983)
- [6] Peng S, Peng L, Yi C, et al. A novel synthetic strategy for preparing semi-aromatic components modified polyamide 6 polymer. *J Polym Sci Part A Polym Chem*. 2018;56(9):959–967. doi: [10.1002/pola.28983](https://doi.org/10.1002/pola.28983)

- [7] García JM, García FC, Serna F, et al. High-performance aromatic polyamides. *Prog Polym Sci*. 2010;35(5):623–686. doi: [10.1016/j.progpolymsci.2009.09.002](https://doi.org/10.1016/j.progpolymsci.2009.09.002)
- [8] Zhang CL, Wan L, Gu XP, et al. A study on a prepolymerization process of aromatic-contained polyamide copolymers PA(66-co-6T) via one-step polycondensation. *Macromol Reaction Eng*. 2015;9(5):512–521. doi: [10.1002/mren.201500006](https://doi.org/10.1002/mren.201500006)
- [9] Zhang G, Yan G-M, Yu T, et al. Semiaromatic polyamides containing carboxyl unit: synthesis and properties. *Ind Eng Chem Res*. 2017;56(33):9275–9284. doi: [10.1021/acs.iecr.7b01998](https://doi.org/10.1021/acs.iecr.7b01998)
- [10] Feng W, Zou G, Ding Y, et al. Effect of aliphatic diacid chain length on properties of semiaromatic copolyamides based on PA10T and Their theoretical study. *Ind Eng Chem Res*. 2019;58(17):7217–7226. doi: [10.1021/acs.iecr.9b01041](https://doi.org/10.1021/acs.iecr.9b01041)
- [11] Zhang G, Yan G-M, Ren H-H, et al. Effects of a trans- or cis-cyclohexane unit on the thermal and rheological properties of semi-aromatic polyamides. *Polym Chem*. 2016;7(1):44–53. doi: [10.1039/c5py01634g](https://doi.org/10.1039/c5py01634g)
- [12] Yagura K, Zhang Y, Enomoto Y, et al. Synthesis of highly thermally stable divanillic acid-derived polyamides and their mechanical properties. *Polymer*. 2021;228. doi: [10.1016/j.polymer.2021.123907](https://doi.org/10.1016/j.polymer.2021.123907)
- [13] Stouten J, Wróblewska AA, Grit G, et al. Polyamides containing a biorenewable aromatic monomer based on coumalate esters: from synthesis to evaluation of the thermal and mechanical properties. *Polym Chem*. 2021;12(16):2379–2388. doi: [10.1039/D1PY00005E](https://doi.org/10.1039/D1PY00005E)
- [14] Murase SK, Franco L, Del Valle LJ, et al. Synthesis and characterization of poly(ester amides)s with a variable ratio of branched odd diamide units. *J Appl Polym Sci*. 2013;131(7). doi: [10.1002/app.40102](https://doi.org/10.1002/app.40102)
- [15] Ramirez MA, Corona MV, Blanco MM, et al. New synthetic route for selectively substituted 1,n-diamines. Synthesis of N-aryl tetra- and pentamethylenediamines. *Tetrahedron Lett*. 2010;51(38):5000–5002. doi: [10.1016/j.tetlet.2010.07.075](https://doi.org/10.1016/j.tetlet.2010.07.075)
- [16] Qian ZG, Xia LS XX, Lee SY. Metabolic engineering of *Escherichia coli* for the production of cadaverine: a five carbon diamine. *Biotechnol Bioeng*. 2010;108(1):93–103. doi: [10.1002/bit.22918](https://doi.org/10.1002/bit.22918)
- [17] Kim H, Yoo HY, Park N, et al. Enhanced L-lysine into 1,5-diaminopentane conversion via statistical optimization of whole-cell decarboxylation system. *Polymers*. 2019;11(8):1372. doi: [10.3390/polym11081372](https://doi.org/10.3390/polym11081372)
- [18] Kim HT, Baritugo K-A, Oh YH, et al. Metabolic engineering of *Corynebacterium glutamicum* for the high-level production of cadaverine that can be used for the synthesis of biopolyamide 510. *ACS Sustain Chem Eng*. 2018;6(4):5296–5305. doi: [10.1021/acssuschemeng.8b00009](https://doi.org/10.1021/acssuschemeng.8b00009)
- [19] Yu G, Liu C, Zhou H, et al. Synthesis and characterization of soluble copoly(arylene ether sulfone phenyl-s-triazine)s containing phthalazinone moieties in the main chain. *Polymer*. 2009;50(19):4520–4528. doi: [10.1016/j.polymer.2009.07.030](https://doi.org/10.1016/j.polymer.2009.07.030)
- [20] Song Y, Wang J, Li G, et al. Synthesis, characterization and optical properties of cross-linkable poly(phthalazinone ether ketone sulfone). *Polymer*. 2008;49(3):724–731. doi: [10.1016/j.polymer.2007.12.015](https://doi.org/10.1016/j.polymer.2007.12.015)

- [21] C-X F, Huang T, H-M C, et al. Carbon nanotubes induced poly(vinylidene fluoride) crystallization from a miscible poly(vinylidene fluoride)/poly(methyl methacrylate) blend. *Colloid Polym Sci.* 2014;292(12):3279–3290. doi: [10.1007/s00396-014-3375-9](https://doi.org/10.1007/s00396-014-3375-9)
- [22] Suksut B, Deeprasertkul C. Effect of nucleating agents on physical properties of Poly(lactic acid) and its blend with natural rubber. *J Polym Environ.* 2010;19(1):288–296. doi: [10.1007/s10924-010-0278-9](https://doi.org/10.1007/s10924-010-0278-9)
- [23] Hemanth R, Suresha B, Sekar M. Physico-mechanical behaviour of thermoplastic co-polyester elastomer/polytetrafluoroethylene composite with short fibers and microfillers. *J Composite Mater.* 2014;49(18):2217–2229. doi: [10.1177/0021998314545183](https://doi.org/10.1177/0021998314545183)
- [24] Meng C, Liu X. Synthesis of bio-based semi aromatic high temperature polyamide PA5T/56 and effect of benzene ring on non-isothermal crystallization kinetics. *J Polym Res.* 2021;28(10). doi: [10.1007/s10965-021-02727-3](https://doi.org/10.1007/s10965-021-02727-3)
- [25] Zhang Y, Cai Z, Wang Y, et al. Effect of sequence distribution on the non-isothermal crystallization of copolyamide 4/6. *J Mater Sci.* 2022;57(37):17883–17901. doi: [10.1007/s10853-022-07709-4](https://doi.org/10.1007/s10853-022-07709-4)
- [26] Liu M, Li K, Yang S, et al. Synthesis and thermal decomposition of poly(dodecamethylene terephthalamide). *J Appl Polym Sci.* 2011;122(5):3369–3376. doi: [10.1002/app.34416](https://doi.org/10.1002/app.34416)
- [27] Wang W, Wang F, Li H, et al. Synthesis of phosphorus-nitrogen hybrid flame retardant and investigation of its efficient flame-retardant behavior in PA6 / PA66. *J Appl Polym Sci.* 2022;140(8). doi: [10.1002/app.53536](https://doi.org/10.1002/app.53536)
- [28] Qiu Z, Chen C, Huang Z, et al. New insights into contribution of aromatic ring versus aliphatic ring to thermal transition temperatures of heat resistant polyamides: a comparison study of PA 10T and t-pa 10C. *Polymer.* 2023;267. doi: [10.1016/j.polymer.2023.125701](https://doi.org/10.1016/j.polymer.2023.125701)
- [29] Aerdt A, Eersels K, Groeninckx G. Transamidation in melt-mixed aliphatic and aromatic polyamides. 1. Determination of the degree of randomness and number-average block length by means of ^{13}C NMR. *Macromolecules.* 1996;29:1041–1045. doi: [10.1021/ma9507857](https://doi.org/10.1021/ma9507857)
- [30] Liu B, Hu G, Zhang J, et al. Non-isothermal crystallization, yellowing resistance and mechanical properties of heat-resistant nylon 10T/66/titania dioxide/glass fibre composites. *RSC Adv.* 2019;9(13):7057–7064. doi: [10.1039/C8RA10037C](https://doi.org/10.1039/C8RA10037C)
- [31] Gao Y, Yang T, Wang X, et al. Synthesis and characterization of poly(hexamethylene terephthalate/hexamethylene oxamide) alternating copolyamide (alt-PA6T /62). *J Appl Polym Sci.* 2020;138(5). doi: [10.1002/app.49773](https://doi.org/10.1002/app.49773)
- [32] Zhu R, Pu Z, Hou H, et al. Effect of copolymerization on the thermal characteristics and behavior of crystallization of biobased semi-aromatic PA10T / 10I. *J Appl Polym Sci.* 2023;140(22). doi: [10.1002/app.53903](https://doi.org/10.1002/app.53903)
- [33] Yang K, Guo Q, Liu Y, et al. Bio-based pentamethylenediamine-derived semiaromatic copolyamide: controllable synthesis and discoloration mechanism. *Ind Eng Chem Res.* 2022. doi: [10.1021/acs.iecr.2c03020](https://doi.org/10.1021/acs.iecr.2c03020)
- [34] Sun Z, Wang X, Guo F, et al. Isothermal and nonisothermal crystallization kinetics of bio-sourced nylon 69. *Chin J Chem Eng.* 2016;24(5):638–645. doi: [10.1016/j.cjche.2015.12.021](https://doi.org/10.1016/j.cjche.2015.12.021)
- [35] Wang Y, Kang HL, Wang R, et al. Crystallization of polyamide 56/polyamide 66 blends: non-isothermal crystallization kinetics. *J Appl Polym Sci.* 2018;135(26). doi: [10.1002/app.46409](https://doi.org/10.1002/app.46409)
- [36] Sun X, Mai K, Zhang C, et al. Nonisothermal crystallization kinetics of bio-based semi-aromatic polyamides. *J Therm Anal Calorim.* 2017;130(2):1021–1030. doi: [10.1007/s10973-017-6434-x](https://doi.org/10.1007/s10973-017-6434-x)
- [37] Wan X, Zhang K, Yin Z, et al. Non-isothermal crystallization kinetics of ethylene-tetrafluoroethylene copolymer using integral avrami equation. *J Polym Eng.* 2023;43(3):210–218. doi: [10.1515/polyeng-2022-0204](https://doi.org/10.1515/polyeng-2022-0204)
- [38] Rozwadowski T, Jasiurkowska-Delaporte M, Massalska-Arodz M, et al. Designing the disorder: the kinetics of nonisothermal crystallization of the orientationally disordered crystalline phase in a nematic mesogen. *Phys Chem Chem Phys.* 2020;22(42):24236–24248. doi: [10.1039/D0CP04002A](https://doi.org/10.1039/D0CP04002A)
- [39] Ahmed J, Luciano G, Maggiore S. Nonisothermal crystallization behavior of polylactide/polyethylene glycol/graphene oxide nanosheets composite films. *Polym Compos.* 2020;41(5):2108–2119. doi: [10.1002/pc.25524](https://doi.org/10.1002/pc.25524)
- [40] Somrang N, Nithitanakul M, Grady BP, et al. Non-isothermal melt crystallization kinetics for ethylene-acrylic acid copolymers and ethylene-methyl acrylate-acrylic acid terpolymers. *Eur Polym J.* 2004;40(4):829–838. doi: [10.1016/j.eurpolymj.2003.11.021](https://doi.org/10.1016/j.eurpolymj.2003.11.021)
- [41] Macedo TCP, Campos DAT, Lima TN, et al. Non-isothermal crystallization kinetics, thermal, and rheological behavior of linear/branched polypropylene blends. *Macromol Symposia.* 2022;406(1). doi: [10.1002/masy.202200042](https://doi.org/10.1002/masy.202200042)